

## Room-Temperature and Near-Room-Temperature Molecule-Based Magnets

Mark D. Harvey, T. Daniel Crawford, and Gordon T. Yee\*

Department of Chemistry, Virginia Polytechnic Institute and State University, Blacksburg, Virginia 24061

Received December 3, 2007

Additional members of the family of high- $T_c$  molecule-based magnets,  $V[\text{acceptor}]_2 \cdot y\text{CH}_2\text{Cl}_2$  have been discovered in which the acceptor is a fluorophenyltricyanoethylene. Varying the number and position of the fluorine substitutions around the phenyl ring results in materials with significantly different magnetic ordering temperatures ( $T_c$ 's) ranging from 160 to 300 K. Density functional theory calculations were performed on the neutral and anionic forms of the acceptors that reveal modest correlation between  $T_c$  and three calculated quantities: the gas-phase electron affinity, the dihedral angle between the phenyl ring and the olefin, and the Mulliken spin densities on the nitrogen atoms. The electrochemistry of the acceptors has also been examined.

### Introduction

Ferrimagnetic  $V[\text{TCNE}]_2 \cdot y\text{CH}_2\text{Cl}_2$  is an air-sensitive, amorphous black molecule-based solid that is magnetically ordered below  $\sim 390$  K.<sup>1</sup> Although the compound has been known for over a decade, relatively little is understood about how it functions as a ferrimagnet. The structure is believed to be a network of  $d^3$   $V^{II}$  ions in a coordination environment with bridging TCNE radical anions. Miller and co-workers have shown that reactions between  $\text{MI}_2 \cdot y\text{CH}_3\text{CN}$  ( $M = \text{Mn}, \text{Fe}, \text{Co}, \text{or Ni}$ ) and TCNE provide magnetically ordered solids similar to  $V[\text{TCNE}]_2$  but with  $T_c$ 's between 44 and 121 K.<sup>2</sup> In an analogous work, we<sup>3–5</sup> and others<sup>6–8</sup> have reacted other organic one-electron acceptors with  $V(\text{CO})_6$  to give additional examples of vanadium-based magnets. However, what has been lacking is an examination of closely related substitutes for TCNE that would allow us to incrementally

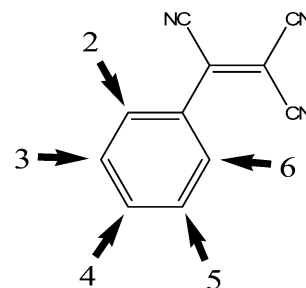


**Figure 1.** Numbering scheme for the  $x$ -FPTCE acceptors. Note the equivalence of positions 2 and 6 and positions 3 and 5 assuming free rotation about the bond connecting the olefin to the phenyl ring.

and systematically vary the steric and electronic properties of the resulting acceptors with the goal of uncovering the mechanism of magnetic ordering in these compounds and designing additional room-temperature magnets. The results of the first of several such studies are presented.

In particular, here we report the synthesis and properties of new ferrimagnets constructed from six related acceptors in which we have replaced one or more phenyl hydrogen atoms with a fluorine atom to produce nominally isosteric acceptors: the 2-fluoro-, 3-fluoro-, 4-fluoro-, 2,4-difluoro-, 2,6-difluoro-, and 3,5-difluorophenyltricyanoethylenes (Figures 1 and 2), which are intermediate between the previously reported phenyltricyanoethylene ( $T_c = 215$  K) and pentafluorophenyltricyanoethylene ( $T_c = 307$  K).<sup>5</sup> Attempts were made to correlate the observed ordering temperatures with computed and experimentally determined properties of the eight acceptors, with some limited success. The properties

\* To whom correspondence should be addressed. E-mail: gyee@vt.edu.

- (1) Manriquez, J. M.; Yee, G. T.; McLean, R. S.; Epstein, A. J.; Miller, J. S. *Science* **1991**, *252*, 1415–1417.
- (2) Zhang, J.; Enslin, J.; Ksenofontov, V.; Gütllich, P.; Epstein, A. J.; Miller, J. S. *Angew. Chem., Int. Ed.* **1998**, *37*, 657–660.
- (3) Fitzgerald, J. P.; Kaul, B. B.; Yee, G. T. *Chem. Commun.* **2000**, 49–50.
- (4) Kaul, B. B.; Yee, G. T. *Inorg. Chem. Acta* **2001**, *326*, 9–12.
- (5) Harvey, M. D.; Pace, J. T.; Yee, G. T. *Polyhedron* **2007**, *26*, 2037–2041.
- (6) Vickers, E. B.; Selby, T. D.; Thorum, M. S.; Taliaferro, M. L.; Miller, J. S. *Inorg. Chem.* **2004**, *43*, 6414–6420.
- (7) Vickers, E. B.; Selby, T. D.; Miller, J. S. *J. Am. Chem. Soc.* **2004**, *126*, 3716–3717.
- (8) Taliaferro, M. L.; Thorum, M. S.; Miller, J. S. *Angew. Chem., Int. Ed.* **2006**, *45*, 5326–5331.

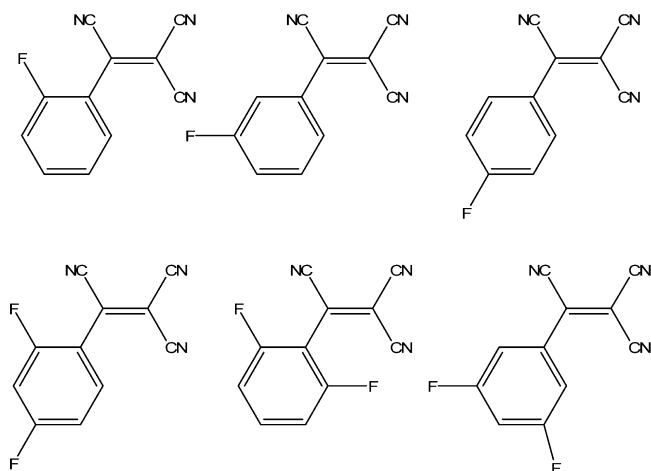


**Figure 2.** Mono- and disubstituted acceptors from left to right and then top to bottom: 2-fluoro-, 3-fluoro-, 4-fluoro-, 2,4-difluoro-, 2,6-difluoro-, and 3,5-difluorophenyltricyanoethylene.

we have examined include the calculated gas-phase electron affinity (EA), the dihedral angle between the phenyl ring and the olefin, and the experimentally determined first reduction potential. It is noteworthy that essentially by design the 2,6-difluoro compound was synthesized and it yields a new room-temperature magnet.

## Experimental Section

**Materials and General Considerations.** Preparations of air-sensitive compounds were carried out in a nitrogen-filled Vacuum Atmospheres glovebox.  $[(Et)_4N]^+[V(CO)_6]^-$  and subsequently vanadium hexacarbonyl were prepared according to a literature procedure.<sup>9</sup> Malononitrile, *N*-chlorosuccinimide, sodium cyanide, potassium cyanide, and piperidine were purchased from Aldrich. All fluorinated benzaldehydes were purchased from Acros. Reagents were used as received except as noted below. Dichloromethane was distilled from  $P_2O_5$  and degassed with glovebox nitrogen prior to use. Acetonitrile was distilled from  $P_2O_5$ , followed by distillation from  $CaH_2$  under argon prior to use. All fluorinated acceptors were synthesized based on a modified literature procedure<sup>10</sup> and described below. Elemental analyses were performed by Desert Analytics, Tucson, AZ.

**Magnetic Measurements.** All magnetic measurements were performed on a 7 T Quantum Design MPMS SQUID magnetometer. Measurements of field-cooled magnetization as a function of the temperature were performed from 5 to 300 or 310 K as indicated. Powder samples were cooled in a 100 G applied field and measured upon warming in a 5 G applied field. Measurements of magnetization as a function of the applied magnetic field were performed at 5 K. The amplitude of the oscillating magnetic field used for alternating current (ac) susceptibility measurements was 3.5 Oe with a zero direct current bias field and at frequencies of 1, 10, and 100 Hz. Diamagnetic corrections were not applied to the  $M$  vs  $T$  or  $M$  vs  $H$  data.

**Electrochemistry Measurements.** The cyclic voltammograms were recorded using a CH Instruments model 600A potentiostat. Measurements were performed on  $\sim 5$  mM solutions in  $CH_3CN/0.1$  M  $[n-Bu_4N][PF_6]$  and taken between the potential range of 0

and  $-400$  mV at a scan rate of 100 mV/s using a polished carbon electrode with Ag/AgCl as the reference. Solution resistance was compensated 95% using positive-feedback IR compensation for all measurements.

**Powder Diffraction Measurements.** Samples were sealed in 1.0 mm diameter glass capillaries (Blake Industries, Scotch Plains, NJ) inside the glovebox, and data were collected in transmission mode on an R-Axis Rapid diffractometer using copper radiation, a graphite monochromator, and a 0.5 mm incident beam collimator.

**Density Functional Theory (DFT) Calculations.** EA calculations were performed using the B3LYP density functional with the 6-31++G\*\* basis set within *Gaussian03*.<sup>11</sup> Starting from the geometrically optimized  $H_3PTCE$  (unsubstituted acceptor), both the optimized neutral and anionic forms of each fluorinated acceptor were calculated. From the results of the geometry optimizations, acceptor energies (both neutral and anionic) and Mulliken spin densities were collected.

**Synthesis of 2-(2-Fluorophenyl)-1,1-dicyanoethylene.** In a 250 mL beaker, 2-fluorobenzaldehyde (6.35 g, 51.2 mmol) and malononitrile (3.38 g, 51.2 mmol) were stirred together with a magnetic stirbar and dissolved in  $\sim 150$  mL of 100% ethanol. While stirring, 1 drop of piperidine was added. After further stirring for  $\sim 10$  min, the stirbar was removed and the beaker was transferred to the refrigerator and left overnight. The white crystals that resulted were collected by filtration, rinsed thoroughly with ice-cold 95% ethanol, and dried by suction. Yield: 7.44 g (84%). IR (KBr):  $\nu_{C\equiv N}$  2229 and 2225  $cm^{-1}$ .  $^1H$  NMR (400 MHz,  $CDCl_3$ , vs TMS):  $\delta$  8.28 (t, 1H), 8.10 (s, 1H), 7.64 (m, 1H), 7.34 (t, 1H), 7.23 (t, 1H).  $^{19}F$  NMR (376 MHz,  $CDCl_3$  vs Freon 11 (external standard)):  $\delta$   $-111.4$  (s, 1F).

**Synthesis of 2-(2-Fluorophenyl)-1,1,2-tricyanoethane.** In a 1 L Erlenmeyer flask, 2-(2-fluorophenyl)-1,1-dicyanoethylene (6.42 g, 37.3 mmol) was dissolved in  $\sim 300$  mL of 100% ethanol. The solution was then cooled in an ice bath. Separately, potassium cyanide (4.95 g, 76.1 mmol) was dissolved in  $\sim 150$  mL of water and also cooled in an ice bath. In quick succession, the cold potassium cyanide solution was added to the ethanol solution followed by  $\sim 500$  mL of ice-cold water. After stirring for 1 h, 10 mL of concentrated HCl was added dropwise to precipitate a white solid. After stirring for another 30 min, the stirbar was removed and the flask was transferred to the refrigerator overnight to allow the solid to settle. The white crystals were filtered, rinsed thoroughly with water, and dried by suction. Yield: 6.21 g (84%). IR (KBr):  $\nu_{C\equiv N}$  2259, 2254, and 2250  $cm^{-1}$ .  $^1H$  NMR (400 MHz,  $CDCl_3$ , vs TMS):  $\delta$  7.69 (t, 1H), 7.55 (m, 1H), 7.37 (t, 1H), 7.24 (t, 1H), 4.83 (d, 1H), 4.31 (d, 1H).  $^{19}F$  NMR (376 MHz,  $CDCl_3$  vs Freon 11 (external standard)):  $\delta$   $-116.9$  (s, 1F).

**Synthesis of 2-(2-Fluorophenyl)-1,1,2-tricyanoethylene (2-FPTCE).** In a 1 L round-bottomed flask equipped with a magnetic stirbar, 2-(2-fluorophenyl)-1,1,2-tricyanoethane (4.6 g, 23 mmol) was dissolved in  $\sim 300$  mL of diethyl ether. *N*-Chlorosuccinimide (4.63 g, 34.8 mmol) was added to the solution. Then  $\sim 200$  mL of ice-cold water was poured into the flask, and the two-phase mixture was stirred vigorously for 1 h. The mixture was transferred to a separatory funnel and the aqueous layer discarded. The organic layer was washed with water ( $3 \times 150$  mL), dried with anhydrous sodium sulfate, filtered, and finally removed in vacuo to afford a light-yellow solid. The final product was then purified by silica gel

(9) Liu, X.; Ellis, J. E.; Miller, T. D.; Ghalasi, P.; Miller, J. S. *Inorg. Synth.* **2004**, *34*, 96–103.

(10) Corson, B. B.; Stoughton, R. W. *J. Am. Chem. Soc.* **1928**, *50*, 2825–2837.

(11) Frisch, M. J.; et al. *Gaussian03*, revision C.02; Gaussian, Inc.: Wallingford, CT, 2004.

(12) Haskel, D.; Islam, Z.; Lang, J.; Kmety, C.; Srajer, G.; Pokhodnya, K. I.; Epstein, A. J.; Miller, J. S. *Phys. Rev. B: Condens. Matter* **2004**, *70* (054422), 1–9.

column chromatography with a dichloromethane mobile phase. Yield: 3.26 g (72%). Mp: 106.0–106.5 °C. IR (KBr):  $\nu_{\text{C}\equiv\text{N}}$  2237 and 2235  $\text{cm}^{-1}$ .  $^1\text{H}$  NMR (400 MHz,  $\text{CDCl}_3$ , vs TMS):  $\delta$  7.72 (m, 1H), 7.68 (m, 1H), 7.41 (t, 1H), 7.34 (t, 1H).  $^{19}\text{F}$  NMR (376 MHz,  $\text{CDCl}_3$ , vs Freon 11 (external standard)):  $\delta$  -105.3 (s, 1F). HRMS-FAB ( $m/z$ , [M]). Calcd for  $\text{C}_{11}\text{H}_4\text{N}_3\text{F}$ : 197.038919. Found: 197.03934.

**Synthesis of V[2-FPTCE]<sub>2</sub>.** Under a nitrogen atmosphere, vanadium hexacarbonyl (25.4 mg, 0.116 mmol) dissolved in dichloromethane (2 mL) was added dropwise to a solution containing 2-FPTCE (65.4 mg, 0.332 mmol) in dichloromethane (2 mL) with stirring. After 25 min, the black precipitate was collected on a medium frit, rinsed with dichloromethane (3 × 2 mL), and dried in vacuo for 1 h. Yield: 53 mg (99%). IR (KBr):  $\nu_{\text{C}\equiv\text{N}}$  2213 and 2130  $\text{cm}^{-1}$ . Anal. Calcd for  $\text{C}_{22}\text{F}_2\text{H}_8\text{N}_6\text{V}_1 \cdot 0.40\text{CH}_2\text{Cl}_2$ : C, 56.17; H, 1.85; N, 17.55. Found: C, 56.16; H, 1.71; N, 17.62.

**Synthesis of 2-(3-Fluorophenyl)-1,1,2-tricyanoethylene (3-FPTCE).** 3-FPTCE was prepared by using a procedure similar to that of 2-FPTCE with 3-fluorobenzaldehyde as the starting material. Yield: 1.58 g (80%). Mp: 99.1–99.5 °C. IR (KBr):  $\nu_{\text{C}\equiv\text{N}}$  2236 and 2231  $\text{cm}^{-1}$ .  $^1\text{H}$  NMR (400 MHz,  $\text{CDCl}_3$ , vs TMS):  $\delta$  7.81 (d, 1H), 7.61–7.72 (m, 2H), 7.45 (t, 1H).  $^{19}\text{F}$  NMR (376 MHz,  $\text{CDCl}_3$ , vs Freon 11 (external standard)):  $\delta$  -107.9 (s, 1F). HRMS-FAB ( $m/z$ , [M]). Calcd for  $\text{C}_{11}\text{H}_4\text{N}_3\text{F}$ : 197.038919. Found: 197.03725.

**Synthesis of V[3-FPTCE]<sub>2</sub>.** V[3-FPTCE]<sub>2</sub> was prepared by using a procedure similar to that of V[2-FPTCE]<sub>2</sub>. Yield: 39.4 mg (95%). IR (KBr):  $\nu_{\text{C}\equiv\text{N}}$  2213 and 2140  $\text{cm}^{-1}$ . Anal. Calcd for  $\text{C}_{22}\text{F}_2\text{H}_8\text{N}_6\text{V}_1 \cdot 0.31\text{CH}_2\text{Cl}_2$ : C, 56.82; H, 1.84; N, 17.82. Found: C, 56.85; H, 2.04; N, 17.65.

**Synthesis of 2-(4-Fluorophenyl)-1,1,2-tricyanoethylene (4-FPTCE).** 4-FPTCE was prepared by using a procedure similar to that of 2-FPTCE with 4-fluorobenzaldehyde as the starting material. Yield: 1.81 g (61%). Mp: 122.6–123.1 °C. IR (KBr):  $\nu_{\text{C}\equiv\text{N}}$  2238 and 2233  $\text{cm}^{-1}$ .  $^1\text{H}$  NMR (400 MHz,  $\text{CDCl}_3$ , vs TMS):  $\delta$  8.08 (m, 2H), 7.33 (m, 2H).  $^{19}\text{F}$  NMR (376 MHz,  $\text{CDCl}_3$ , vs Freon 11 (external standard)):  $\delta$  -97.9 (s, 1F). HRMS-FAB ( $m/z$ , [M]). Calcd for  $\text{C}_{11}\text{H}_4\text{N}_3\text{F}$ : 197.038919. Found: 197.0376.

**Synthesis of V[4-FPTCE]<sub>2</sub>.** V[4-FPTCE]<sub>2</sub> was prepared by using a procedure similar to that of V[2-FPTCE]<sub>2</sub>. Yield: 45.8 mg (91%). IR (KBr):  $\nu_{\text{C}\equiv\text{N}}$  2214 and 2127  $\text{cm}^{-1}$ . Anal. Calcd for  $\text{C}_{22}\text{F}_2\text{H}_8\text{N}_6\text{V}_1 \cdot 0.19\text{CH}_2\text{Cl}_2$ : C, 57.76; H, 1.83; N, 18.21. Found: C, 57.76; H, 2.04; N, 17.82.

**Synthesis of 2-(2,6-Difluorophenyl)-1,1,2-tricyanoethylene (2,6-diFPTCE).** 2,6-diFPTCE was prepared by using a procedure similar to that of 2-FPTCE with 2,6-difluorobenzaldehyde as the starting material. Yield: 0.98 g (78%). Mp: 104.5–104.9 °C. IR (KBr):  $\nu_{\text{C}\equiv\text{N}}$  2250, 2245, and 2237  $\text{cm}^{-1}$ .  $^1\text{H}$  NMR (400 MHz,  $\text{CDCl}_3$ , vs TMS):  $\delta$  7.70 (m, 1H), 7.17 (t, 2H).  $^{19}\text{F}$  NMR (376 MHz,  $\text{CDCl}_3$ , vs Freon 11 (external standard)):  $\delta$  -105.2 (s, 2F). HRMS-FAB ( $m/z$ , [M]). Calcd for  $\text{C}_{11}\text{H}_3\text{N}_3\text{F}_2$ : 215.029500. Found: 215.02991.

**Synthesis of V[2,6-diFPTCE]<sub>2</sub>.** V[2,6-diFPTCE]<sub>2</sub> was prepared by using a procedure similar to that of V[2-FPTCE]<sub>2</sub>. Yield: 47.8 mg (94%). IR (KBr):  $\nu_{\text{C}\equiv\text{N}}$  2197 and 2134  $\text{cm}^{-1}$ . Anal. Calcd for  $\text{C}_{22}\text{F}_4\text{H}_6\text{N}_6\text{V}_1 \cdot 0.54\text{CH}_2\text{Cl}_2$ : C, 51.36; H, 1.35; N, 15.94. Found: C, 51.36; H, 1.31; N, 16.12.

**Synthesis of 2-(3,5-Difluorophenyl)-1,1,2-tricyanoethylene (3,5-diFPTCE).** 3,5-diFPTCE was prepared by using a procedure similar to that of 2-FPTCE with 3,5-difluorobenzaldehyde as the starting material. Yield: 1.34 g (67%). Mp: 109.6–109.9 °C. IR (KBr):  $\nu_{\text{C}\equiv\text{N}}$  2241 and 2235  $\text{cm}^{-1}$ .  $^1\text{H}$  NMR (400 MHz,  $\text{CDCl}_3$ , vs TMS):  $\delta$  7.54 (m, 2H), 7.21 (m, 1H).  $^{19}\text{F}$  NMR (376 MHz,  $\text{CDCl}_3$ , vs Freon 11 (external standard)):  $\delta$  -103.8 (s, 2F). HRMS-FAB ( $m/z$ , [M]). Calcd for  $\text{C}_{11}\text{H}_3\text{N}_3\text{F}_2$ : 215.029500. Found: 215.03026.

**Synthesis of V[3,5-diFPTCE]<sub>2</sub>.** V[3,5-diFPTCE]<sub>2</sub> was prepared by using a procedure similar to that of V[2-FPTCE]<sub>2</sub>. Yield: 40 mg (90%). IR (KBr):  $\nu_{\text{C}\equiv\text{N}}$  2205 and 2138  $\text{cm}^{-1}$ . Anal. Calcd for  $\text{C}_{22}\text{F}_4\text{H}_6\text{N}_6\text{V}_1$ : C, 54.91; H, 1.26; N, 17.46. Found: C, 54.99; H, 1.42; N, 17.17.

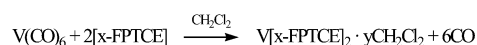
**Synthesis of 2-(2,4-Difluorophenyl)-1,1,2-tricyanoethylene (2,4-diFPTCE).** 2,4-diFPTCE was prepared by using a procedure similar to that of 2-FPTCE with 2,4-difluorobenzaldehyde as the starting material. Yield: 1.50 g (75%). Mp: 72.6–73.1 °C. IR (KBr):  $\nu_{\text{C}\equiv\text{N}}$  2229 and 2225  $\text{cm}^{-1}$ .  $^1\text{H}$  NMR (400 MHz,  $\text{CDCl}_3$ , vs TMS):  $\delta$  8.08 (m, 2H), 7.33 (m, 2H).  $^{19}\text{F}$  NMR (376 MHz,  $\text{CDCl}_3$ , vs Freon 11 (external standard)):  $\delta$  -97.9 (s, 1F). HRMS-FAB ( $m/z$ , [M]). Calcd for  $\text{C}_{11}\text{H}_3\text{N}_3\text{F}_2$ : 215.029500. Found: 215.0294.

**Synthesis of V[2,4-diFPTCE]<sub>2</sub>.** V[2,4-diFPTCE]<sub>2</sub> was prepared by using a procedure similar to that of V[2-FPTCE]<sub>2</sub>. Yield: 29.7 mg (92%). IR (KBr):  $\nu_{\text{C}\equiv\text{N}}$  2220 and 2132  $\text{cm}^{-1}$ . Anal. Calcd for  $\text{C}_{22}\text{F}_4\text{H}_6\text{N}_6\text{V}_1 \cdot 0.31\text{CH}_2\text{Cl}_2$ : C, 52.81; H, 1.31; N, 16.56. Found: C, 52.81; H, 1.20; N, 16.30.

## Results and Discussion

The synthesis of the desired acceptors (Figure 2) is easily achieved in three steps in moderate yield from commercially available starting materials. Purity was determined by  $^1\text{H}$  and  $^{19}\text{F}$  NMR, mass spectrometry, and melting point measurements. The subsequent reaction of each acceptor in dichloromethane with vanadium hexacarbonyl under a nitrogen atmosphere yields the magnetic material as an insoluble precipitate that cannot be redissolved and that decomposes rapidly when exposed to air. On the basis of elemental analyses, formulas for the six coordination polymers suggest a 1:2 vanadium(II)-to-acceptor ratio with small varying amounts of solvents of crystallization, which are required to agree with the elemental analysis data. This stoichiometry is consistent with that observed for all previous compounds of this type.<sup>3–8</sup> Generally, the number of solvent molecules required for an acceptable fit ( $\nu$ ) was much less than 1. For the sake of simplicity, solvent will not be included in subsequent formulas. Scheme 1 illustrates the general reaction for the preparation of the magnetic phases discussed in this paper, where  $x$  is (are) the position(s) of fluorine atom(s) around the phenyl ring.

**Scheme 1.** Chemical Reaction for the Preparation of V[ $x$ -FPTCE]<sub>2</sub> Magnetic Phases



The structures of these air-sensitive coordination polymers are assumed to be disordered networks of  $\text{V}^{\text{II}}$  cations bridged by two or three of the nitrile groups on the acceptors. All powder diffraction measurements to date show their structures to be amorphous like all other compounds in this family. However, a study involving XANES/EXAFS suggests that the  $\text{V}^{\text{II}}$  ion, within the related V[TCNE]<sub>2</sub> amorphous network, is surrounded by roughly six nitrile nitrogens, creating a pseudo-octahedral coordination environment.<sup>12</sup>

The IR spectrum of each magnet exhibits  $\nu_{\text{C}\equiv\text{N}}$  stretching frequencies consistent with the reduction of the acceptors to the radical anionic state compared to the neutral, uncoordinated acceptors shown in Table 1. All polymer  $\text{C}\equiv\text{N}$  stretches were generally broad, suggesting that several

**Table 1.** Summary of CN Stretching Frequency Data for the Neutral Acceptors and Resulting Magnets<sup>5</sup>

acceptor	acceptor $\nu_{\text{C}\equiv\text{N}}$ , $\text{cm}^{-1}$	polymer $\nu_{\text{C}\equiv\text{N}}$ , $\text{cm}^{-1}$
H <sub>3</sub> PTCE <sup>a</sup>	2235, 2233 (s)	2210, 2129
2-FPTCE	2237 (br), 2235 (s)	2213, 2130
3-FPTCE	2236 (br), 2231 (s)	2213, 2140
4-FPTCE	2238, 2233 (s)	2214, 2127
2,6-diFPTCE	2250, 2245, 2237	2197, 2134
2,4-diFPTCE	2246 (s), 2238	2220, 2132
3,5-diFPTCE	2241, 2235 (s)	2205, 2138
F <sub>3</sub> PTCE <sup>a</sup>	2248, 2238	2201, 2140

<sup>a</sup> Previous work.

environments exist for the reduced acceptors, another defining feature of these types of magnets.<sup>6,13</sup>

The field-cooled magnetization versus temperature data,  $M(T)$ , was obtained promptly after the V[*x*-FPTCE]<sub>2</sub> polymers were synthesized. The  $T_c$ 's were estimated from extrapolation of the steep linear portion of the  $M(T)$  curves. The  $T_c$  values determined by the onset of a nonzero out-of-phase,  $\chi''(T)$ , component of ac susceptibility at 1, 10, and 100 Hz (see the Supporting Information), were slightly lower. The results are summarized in Table 2, and the plots of  $M(T)$  are in Figure 3. The reported  $T_c$  values are the average values for at least two repeat preparations, with ranges noted in column 3.

The magnetization decreases slowly as the sample is warmed from 5 K to well below  $T_c$  and then more rapidly as  $T_c$  is approached. The relatively sharp transition at  $T_c$  suggests some degree of structural and magnetic uniformity throughout the polymers. The  $T_c$ 's of the magnets range from 160 K to around room temperature, 300 K, with high reproducibility and an interesting dependence on the position of the fluorine substitution. Of the monosubstituted species, substitution in the 2 position, closest to the olefin, results in the largest increase in  $T_c$  ( $T_c = 257$  K) relative to the unsubstituted phenyl ring ( $T_c = 215$  K).<sup>5</sup> The 3 position results in a smaller, but still significant increase in  $T_c$  ( $T_c = 233$  K). Quite surprisingly, (vide infra) substitution at the 4 position results in a depression in  $T_c$  ( $T_c = 160$  K).

Furthermore, the effects of the locations of the substitutions around the ring appear to be qualitatively additive. For example, the 2,4-disubstituted acceptor yields a magnet with  $T_c$  between that of the 2- and 4-monosubstituted species. For obtaining high ordering temperatures, the acceptor bearing substitution at both the 3 position and the equivalent 5 position was prepared and it yields a magnet, V[3,5-diFPTCE]<sub>2</sub>, with a  $T_c$  at around 263 K. We expected the highest  $T_c$  of the disubstituted compounds to be exhibited by V[2,6-diFPTCE]<sub>2</sub>, and this is indeed what is observed.

We observe some slight decrease in  $T_c$  with storage of the samples over time, even under vacuum. In one example, V[2,6-diFPTCE]<sub>2</sub>, the  $T_c$  decreased  $\sim 13$  K over the course of 3 months and then remained steady around 287 K. The exact nature of  $T_c$  suppression is unknown but may be related

to the reaction of V<sup>II</sup> with residual solvent. A further discussion of the variation in  $T_c$  for TCNE compounds appears in a recent publication.<sup>14</sup>

Measurements of magnetization versus applied field,  $M(H)$ , were made on each material at 5 K. The results are summarized in Table 2, and a representative sample is plotted in Figure 4 (also in the Supporting Information). Overall, the coercivities are  $\sim 5$  G, which is consistent with a <sup>4</sup>A ground state due to the d<sup>3</sup> configuration of V<sup>II</sup> in a pseudo-octahedral or lower-symmetry crystal field (vide infra). Remanent magnetizations were generally small, usually less than 500 emu·G/mol. Moreover, the magnetization essentially reaches saturation in an applied field of 100 G. Saturation values ranged from 4790 to 5468 emu·G/mol, slightly lower than the ideal value of 5585 emu·G/mol (assuming  $g = 2$ ) for  $S = 3/2$  V<sup>II</sup> antiferromagnetically coupled to two  $S = 1/2$  acceptors (in the formula unit) and far smaller than  $\sim 28\,000$  emu·G/mol expected for ferromagnetic coupling, thereby substantiating each material's existence as a ferrimagnet. The lowered saturation magnetization might be a result of the formation of diamagnetic acceptor dimers, [*x*-FPTCE]<sub>2</sub><sup>2-</sup>, analogous to the diamagnetic [TCNE]<sub>2</sub><sup>2-</sup> unit found in model compounds.<sup>15,16</sup>

Verdaguer and co-workers have rationalized the increased strength of coupling in the Prussian Blue because analogs that involve metal ions further to the left in the periodic table with an orbital overlap model.<sup>17</sup> The higher energy metal d orbitals in V<sup>II</sup> and Cr<sup>III</sup> are believed to be better able to overlap with the empty  $\pi^*$  molecular orbital on the cyanide ligand, leading to the highest  $T_c$ . In the present family of compounds, the V<sup>II</sup> ions may be assumed to reside in an octahedral environment; thus, the metal valence electrons would half-fill the  $t_{2g}$  set with a higher energy  $\pi^*$  orbital located on the reduced acceptor being singly occupied (Figure 5). Carlegrim and co-workers have examined V[TCNE]<sub>2</sub> by NEXAFS and photoelectron spectroscopy and place the TCNE radical anion  $\pi^*$  singly occupied molecular orbital (SOMO) roughly at the same energy as the  $t_{2g}$  orbitals on V<sup>II</sup>.<sup>18</sup> Because by electrochemistry the acceptors reported here are poorer than TCNE, the placement of the *x*-PTCE acceptor  $\pi^*$  SOMO above that of the vanadium orbitals in Figure 5 seems justified. Because the metal d-orbital energy is fixed, when the Verdaguer model is applied, a correlation might be expected between the energy of an acceptor's SOMO and the  $T_c$  of the synthesized polymer. As the SOMO energy approaches that of the vanadium  $t_{2g}$ , better energy matching should lead to greater orbital overlap. In terms of the acceptors described herein, electron-withdrawing fluorine should help to stabilize the SOMO by induction. A larger  $\Delta E$  (better overlap) presumably correlates with a larger

(13) Vickers, E. B.; Giles, I. D.; Miller, J. S. *Chem. Mater.* **2005**, *17*, 1667–1672.(14) Thorum, M. S.; Pokhodnya, K. I.; Miller, J. S. *Polyhedron* **2006**, *25*, 1927–1930.(15) Wang, G.; Zhu, H.; Fan, J.; Sleboznick, C.; Yee, G. T. *Inorg. Chem.* **2006**, *45*, 1406–1408.(16) Novoa, J. J.; Ribas-Arino, J.; Shum, W. W.; Miller, J. S. *Inorg. Chem.* **2007**, *46*, 103–107.(17) Ferlay, S.; Mallah, T.; Ouahès, R.; Veillet, P.; Verdaguer, M. *Nature* **1995**, *378*, 701–703.(18) Carlegrim, E.; Kancierzewska, A.; de Jong, M. P.; Tengstedt, C.; Fahlman, M. *Chem. Phys. Lett.* **2008**, *452*, 173–177.

**Table 2.** Summary of the Magnetic Properties for  $V[x\text{-FPTCE}]_2$  Magnets<sup>a,5</sup>

acceptor	$T_c$ , K	deviation in $T_c$ , K	no. of measurements	$M_s$ , emu·G/mol	$H_{cr}$ , emu·G/mol	$E_{1/2}$ , V	EA, eV	anion dihedral angle, deg
H <sub>5</sub> PTCE <sup>b</sup>	213	±2.5	2	5060	2	-0.40	2.560	15.38
2-FPTCE	257	±1	2	4919	5	-0.35	2.578	38.38
3-FPTCE	233	±3	2	5468	5	-0.30	2.738	13.15
4-FPTCE	160	±2.5	2	4790	5	-0.38	2.655	15.34
2,6-diFPTCE	300	±2.5	4	4852	5	-0.30	2.639	47.10
2,4-diFPTCE	242	±2.5	2	4860	5	-0.34	2.677	40.06
3,5-diFPTCE	263	±1	2	5210	1	-0.22	2.922	11.82
F <sub>5</sub> PTCE <sup>b</sup>	306	±1	2	4190	5	-0.16	3.039	46.48

<sup>a</sup>  $M(H)$  measurements were taken at 5 K. Acceptor redox potentials, relative to Ag/AgCl, were measured in acetonitrile with  $[\text{Bu}_4\text{N}]^+[\text{PF}_6]^-$  as the electrolyte. EAs and anion dihedral angles are calculated gas-phase quantities using *Gaussian03*<sup>11</sup> <sup>b</sup> Previous work.

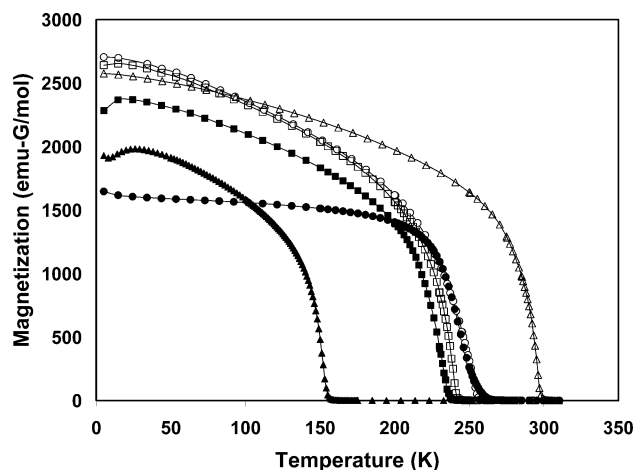


**Figure 3.** Plot of  $M(T)$  measured in a 5 G field for magnets with the formula  $V[x\text{-FPTCE}]_2$ :  $V[2\text{-FPTCE}]_2$  (○),  $V[3\text{-FPTCE}]_2$  (■),  $V[4\text{-FPTCE}]_2$  (▲),  $V[2,6\text{-diFPTCE}]_2$  (△),  $V[2,4\text{-diFPTCE}]_2$  (□), and  $V[3,5\text{-diFPTCE}]_2$  (●).

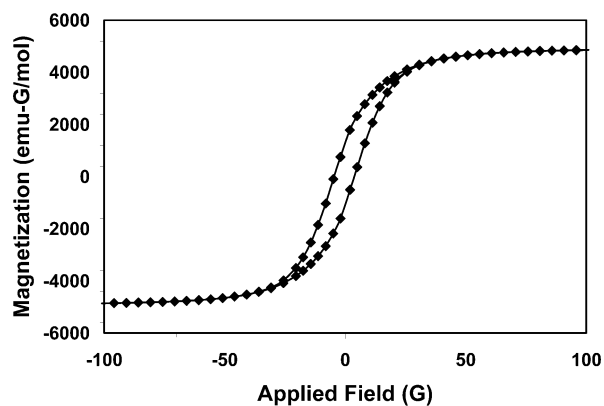


**Figure 4.** Plot of  $M(H)$  for  $V[2,6\text{-diFPTCE}]_2$  at 5 K.

coupling constant,  $J$ , between the unpaired electrons on the metal ion and organic radical. In a mean-field model,  $T_c$  should only depend on  $J$ , assuming the spin and number of nearest neighbors is the same in all of these coordination polymers.<sup>19</sup>

To test this model, we turned to computation, utilizing the B3LYP DFT approach<sup>20,21</sup> and the 6-31++G\*\* basis set using the *Gaussian03* program.<sup>11</sup> The adiabatic EA of the acceptor, which should be directly related to the energy of the SOMO, was calculated by subtracting the radical anion

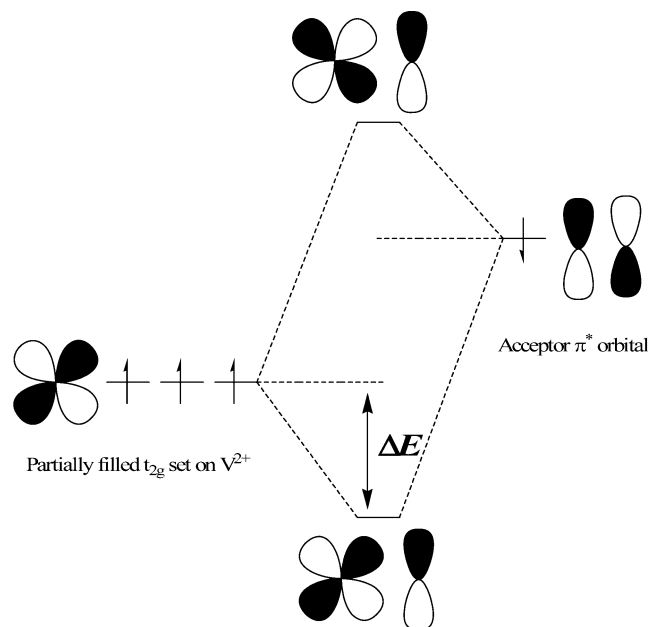


**Figure 5.** Simplified molecular orbital diagram of the assumed interaction between the  $V^{2+}$  d-orbital set and an acceptor  $\pi^*$  orbital in a  $V[x\text{-FPTCE}]_2$  magnetic phase.

B3LYP energy from the neutral acceptor energy using the optimized structure of each species; results are shown in Table 2. (While this approach has been established to provide strong quantitative accuracy for a variety of organic molecules as compared to experimental data,<sup>22</sup> the purpose of this work is to examine only the variation of the EA with the choice of substituents, a task for which the chosen model should be well suited.) Zero-point energy corrections were not included in the EA calculations because their contributions are minimal (about  $\sim 0.05$  eV; see the Supporting Information). The lowest EAs (indicating weaker acceptor ability) were found to be associated with the acceptors with 2 and 2,6 substitutions, followed by 4-FPTCE. The highest EA belongs to the 3,5-diFPTCE acceptor. In the most general terms, there is a correlation between EA and  $T_c$ : acceptors with higher EAs (better acceptors) tend to produce magnets with higher  $T_c$ 's (Figure 6), but the expected simple, predictive, relationship is not borne out. The data do, however, suggest the possible importance of  $\pi$  donation by the fluorine atom when it is in the 2 or 4 position because of the relatively high EA of 3,5-diFPTCE, where  $\pi$  donation is not important. In the 2 position, it could be envisioned

(19) Dixon, D. A.; Suna, A.; Miller, J. S.; Epstein, A. J. In *NATO ARW Molecular Magnetic Materials*; Kahn, O., Gatteschi, D., Miller, J. S., Palacio, F., Eds.; NATO: Brussels, Belgium, 1991; Vol. A198, p 171.

(20) Becke, A. D. *J. Chem. Phys.* **1993**, *98*, 5648–5652.

(21) Lee, C.; Yang, W.; Parr, R. G. *Phys. Rev. B* **1988**, *37*, 785–789.

(22) Rienstra-Kiracofe, J. C.; Tschumper, G. S.; Schaefer, H. F.; Nandi, S.; Ellison, G. B. *Chem. Rev.* **2002**, *102*, 231–282.

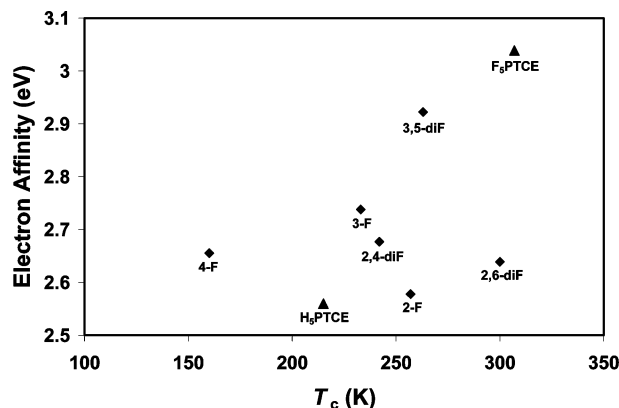


**Figure 6.** Plot of the calculated EA (eV) vs  $T_c$  (K) for the  $V[x\text{-PTCE}]_2$  ( $\blacklozenge$ ) and  $V[\text{H}_3\text{PTCE}]_2/V[\text{F}_3\text{PTCE}]_2$  ( $\blacktriangle$ ) magnets.

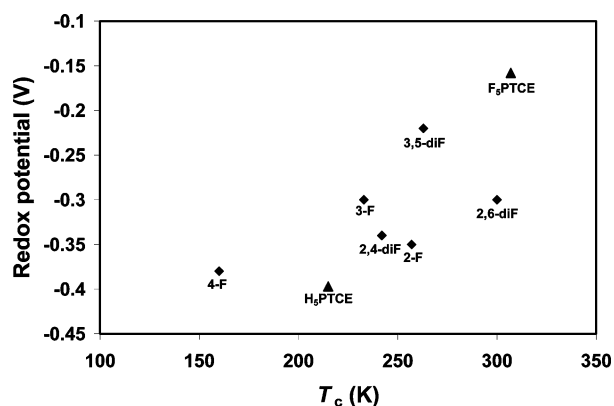


**Figure 7.** Plot of the  $E_{1/2}$  (V) vs  $T_c$ 's (K) for the  $V[x\text{-PTCE}]_2$  ( $\blacklozenge$ ) and  $V[\text{H}_3\text{PTCE}]_2/V[\text{F}_3\text{PTCE}]_2$  ( $\blacktriangle$ ) magnets.

that the inductive effect overwhelms the  $\pi$ -donating effect, but in the 4 position, the inductive effect is substantially decreased. If this explanation were true, we would expect the trend to be reflected in the electrochemical data.

Because it might be argued that the calculated gas-phase EA is not directly relevant, we have also examined the new acceptors by cyclic voltammetry. Table 2 shows the acceptor half-wave potentials versus Ag/AgCl in acetonitrile with tetrabutylammonium hexafluorophosphate as the electrolyte. The most difficult acceptor to reduce was 4-FPTCE with  $E_{1/2} = -0.38$  V, although it is still easier to reduce than the unsubstituted acceptor ( $-0.40$  V), implying that the added fluorine is net electron-withdrawing. The easiest to reduce was 3,5-diFPTCE ( $E_{1/2} = -0.22$  V), which is consistent with the above EA calculations, assuming that solvation energies for all of the compounds are similar. The plot of half-wave potential versus  $T_c$  is shown in Figure 7. If, as expected, the energy of the acceptor  $\pi^*$  orbital (as indicated by the electrochemistry) were a determining factor in the bulk magnetic properties, there should have been a strong correlation between the half-wave potential and the ordering temperature, but once again there is not. While the 3,5 compound has a relatively high  $T_c$ , EA, and redox potential, it does not possess the highest  $T_c$ ; the 2,6 compound has the highest  $T_c$  but is not the easiest to reduce.

Having uncovered no strong correlation between the half-wave potential or EA of the acceptor and the  $T_c$  of the resulting magnet, the distribution of spin density and

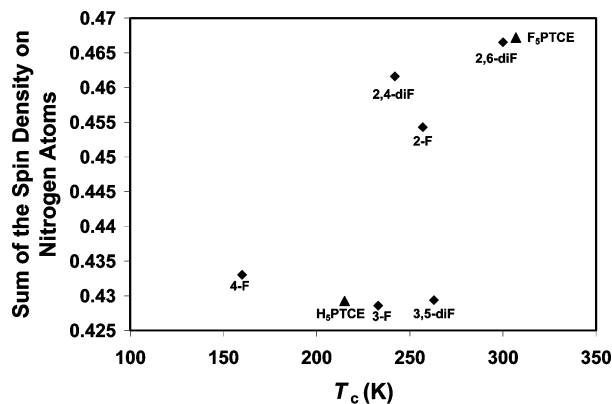


**Figure 8.** Plot of the  $T_c$ 's of the  $V[x\text{-PTCE}]_2$  ( $\blacklozenge$ ) and  $V[\text{H}_3\text{PTCE}]_2$  and  $V[\text{F}_3\text{PTCE}]_2$  ( $\blacktriangle$ ) magnets vs the calculated spin density summed over the nitrile nitrogen atoms using the B3LYP functional and 6-31++G\*\* basis set.

molecular geometry of the anionic acceptors was examined, again using the aforementioned DFT and basis set. With the expectation that the most important spin density is located on the nitrile nitrogen atoms of the acceptors because of their proximity to the vanadium ion, we sought a relationship between that quantity and the  $T_c$  of the polymers. Figure 8 is a plot showing the sum of the spin density on the nitrile nitrogens versus  $T_c$ . In the plot, the data points are separated into two groups distinguished by the presence or absence of substitution in the 2 position. Generally, higher ordering temperatures are associated with greater spin density on the nitrogen atoms, although there is considerable overlap between the two distributions. The most obvious effect of the substitution at the 2 position is rotation about the dihedral angle created by the tricyanovinyl group and the phenyl ring ( $0^\circ = \text{coplanarity}$ ) that arises from interaction of the olefin with a small increase in steric bulk, due to fluorine substitution, at the 2 and/or 6 positions. This twisting decreases the conjugation, localizing the unpaired spin slightly more on the olefin. The plot of  $T_c$  versus the dihedral angle (see the Supporting Information) corroborates this assumption, but again this does not entirely explain the observed trend in  $T_c$ .

However, a combination of steric and electronic effects can, at least qualitatively, explain our observations. In the absence of substitution at the 2 and/or 6 positions, the conjugation between the phenyl ring and the olefin is fairly good and the electronic effects are fairly pronounced. Ordering temperatures span from 160 to 263 K, with reasonable correlation to the redox potential, though it is not clear why fluorine substitution in the 4 position is detrimental. The  $T_c$  difference between the H<sub>3</sub>PTCE and 2-FPTCE magnets is high but is even more dramatic when a second fluorine is added to the 6 position, apparently because of localization of the radical on the olefinic part of the molecule. At low dihedral angle, the magnetic ordering temperatures span a wide range, suggesting a significant electronic influence from the substitution on the ring. However, at the intermediate and highest dihedral angles, the ordering temperatures are more tightly clustered, consistent with the greater importance of a steric effect and the fact that loss of conjugation would make the specific substitution on the phenyl ring less important. This effect is also seen for other

fluorine substitution patterns and for other functional groups that will be discussed in future papers.

### Conclusions

We have expanded the list of acceptors that support magnetic order in reactions with  $V(CO)_6$  to include three monosubstituted and three disubstituted phenyltricyanoethylenes. Ferrimagnets of the general molecular formula  $V[x-FPTCE]_2 \cdot yCH_2Cl_2$ , where  $x$  represents one or more fluorine substitutions and  $y$  is a small fraction generally much less than 1, were synthesized to examine the specific effect of fluorine substitution between the limiting compounds  $V[H_5PTCE]_2$  and  $V[F_3PTCE]_2$  to look for relationships between the electronic properties of the acceptors and observed bulk magnetic ordering temperatures. Magnetic order was realized for all materials, with  $T_c$ 's ranging from 160 to 300 K. On the basis of the magnetic properties of the monosubstituted compounds and the 2,4-disubstituted compound, we targeted the 3,5 and 2,6 compounds, expecting to observe high  $T_c$ 's.

Unfortunately, although we can construct a room-temperature magnet, we have not yet deconvoluted the importance of electronic and steric effects, though both must clearly be playing a role. The highest ordering temperature was exhibited by the magnet derived from  $V[2,6-diFPTCE]_2$ , but this acceptor is not the easiest acceptor to reduce. It does exhibit the largest dihedral angle from the fluorine steric effect, according to the DFT study, which results in the slightly greater localization of spin on the nitrile nitrogen atoms, but the difference in spin density is small. In general, larger dihedral angles correlate with higher ordering tem-

perature. The greater dihedral angle results in a significant loss of conjugation between the olefin and phenyl ring, negating or minimizing the electronic effects of substitution, but this needs to be explored further.

Quite surprisingly, substitution in the 4 position provided a polymer with a  $T_c$  lower than that of the unsubstituted counterpart,  $H_5PTCE$  ( $T_c \sim 215$  K), whereas the dihedral angles are essentially identical. While this might seem to indicate a purely electronic effect in the form of a net electron  $\pi$  donation associated with fluorine in the 4 position, EA calculations and electrochemistry do little to support this explanation. Altogether, these results, nevertheless, suggest empirically that targeting 2,3,5,6-tetrafluorophenyltricyanoethylene might provide a higher  $T_c$  polymer than the pentafluoro analogue, and this will be discussed in a future paper.

**Acknowledgment.** We acknowledge the donors of the Petroleum Research Fund, administered by the American Chemical Society, for support of this work and the National Science Foundation and the Virginia Tech ASPIRES program for partial funding of the purchase of the SQUID magnetometer. We also thank Professors Mark Anderson (Virginia Tech) and Ray Butcher (Howard University) for help with electrochemistry and powder diffraction, respectively.

**Supporting Information Available:** Complete author list for ref 10, magnetic measurements, calculated Mulliken spin densities, and various correlation plots related to EA, redox potential, spin density, dihedral angle, and  $T_c$ 's. This material is available free of charge via the Internet at <http://pubs.acs.org>.

IC702359G